

# SHRINKAGE CRACKING OF SOIL-CEMENT BASE: THEORETICAL AND MODEL STUDIES

K. P. George, University of Mississippi

This paper explores the phenomenon of shrinkage-induced cracking in soil-cement bases. An attempt was made to delineate the primary cause of cracking, and expressions for the shrinkage stresses were derived in accordance with linear viscoelastic theory. The results show that tensile shrinkage stresses are highly localized on the exposed surface. They attain maximum value during the first few days of drying and then decrease rapidly. For quantitative evaluation of shrinkage cracking, however, experiments were conducted on models whose design is based on a dimensional analysis of the linear problem of shrinkage cracking. Experimental results indicate that the crack intensity (defined as area of cracks per unit area) decreases with (a) an increase in the thickness of the slab and (b) a decrease in the viscosity of the material. Adequate extended curing is extremely effective in controlling cracking in cement base. In the 2 coarse-grained and 1 fine-grained soils studied, the crack intensity decreased when the cement content exceeded the ASTM-PCA freeze-thaw criterion. Also, crack intensity tended to decrease with an increase in subgrade friction. In a soil-cement matrix, relatively large pieces of gravel (nominal size  $\frac{1}{2}$  to  $1\frac{1}{4}$  in.) enhanced cracking. The model was used in a search for treatments that led to several promising additives: lime and lime with a trace amount of sugar proved to be best in a variety of soils; expansive cement admixture and sodium silicate surface treatment are effective in coarse-grained soils.

•THE WIDESPREAD phenomenon of cracking in stabilized pavements is generally considered to be caused by a combination of drying shrinkage and ambient temperature during and after the curing period. The fact that cracks may develop in a new pavement before the application of any wheel load indicates the importance of stress caused by changes in temperature and moisture content. Westergaard (32) considered 2 conditions to be involved in this problem. The first arises from slow, uniform shrinkage; the second arises from quick changes of temperature (or drying of a slab from the top) occurring, for example, by the change from a hot day to a cool night and vice versa. Later studies (15, 26, 30) have extended Westergaard's theory to include the effects of a simple harmonic temperature variation, partial support, nonlinear temperature distribution, and viscous damping forces. An obvious conclusion of all these investigations is that warping can induce stresses of sufficient magnitude to cause cracking of concrete highway pavements.

The mechanics of cracks in soil-cement base, or any pavement component for that matter, have not been sufficiently investigated by engineers and researchers. The few studies (19, 25) conducted in this area simply consider the intensity of visible cracking on the pavement surface. As yet, the basic cause of the problem has not been extensively studied. George (7), in a recent paper, presented simplified solutions to crack-spacing and crack-width problems. In that study, the assumption was made that the

material is perfectly elastic. Some implications of a more realistic assumption—that the material is viscoelastic—are discussed in a second paper (10); and in yet another, the cracking problem is examined in accordance with the theory of brittle fracture advanced by Griffith (12). In the present paper, the cracking problem is studied by employing models whose design is based on a dimensional analysis of the linear problem of shrinkage cracking.

The primary objectives are to investigate the mechanics of shrinkage cracking and to delineate the factors influencing the cracking of stabilized soil-cement bases. Whereas some qualitative results are obtained by a theoretical analysis, for quantitative information this investigation utilizes the techniques of dimensional analysis and small-scale model experiments. These models are employed in a further objective of investigating the effectiveness of additives in reducing the shrinkage cracks in soil-cement base.

### STRESS ANALYSIS OF PAVEMENT BASE SUBJECTED TO RESTRAINED SHRINKAGE

An investigation of the shrinkage-induced cracking of pavement base entails the following steps: (a) stress analysis of the slab bonded to the subgrade and shrunk by drying from the top face and (b) determination of a suitable failure criterion. A failure criterion based on ultimate tensile strength is reasonably practical (16) and, hence, will not be discussed here. The first step mentioned, however, is regarded to be so complex a problem that a review of the existing experimental and analytical solutions can be enlightening.

#### Stress Arising From Base-Subgrade Interaction

In a completely constrained pavement slab, a uniform shrinkage will give rise to uniform stress throughout the depth of the slab without any distortion. If the slab is only partially constrained, however, or is subjected to nonlinear strain variation throughout the depth, it will tend to warp. In many instances, warping stresses can be sufficiently high to cause cracking of the slab.

#### Stresses Due to Warping

If a pavement slab is subjected to a temperature gradient, or to a moisture gradient that results from drying from the top face, its surface will tend to warp. For a linear strain distribution, Westergaard (32) solved the problem for a slab of finite width and infinite length, supported on a Winkler foundation. Considering that warping due to nonlinear temperature variation may result in only partial support of the slab by the ground and assuming that subgrade reactions are time-dependent, Reddy, Leonards, and Harr (26) presented expressions for stresses and deflections in a finite circular slab.

#### Stresses Due to Restraint

When a material expands or contracts uniformly but is not allowed to do so at some parts of its boundaries, a phenomenon of restrained shrinkage occurs. In the pavement-cracking problem, the underlying subgrade offers the restraint to the shrinking base. So far, solutions for only 2 limiting cases of restraint are available (4, 31). They are reviewed in the next section.

Stress in a Slab When Bonded on One Face to a Rigid Plate and Shrunk—Assume a hypothetical case of a plate perfectly bonded to a foundation and shrunk. Let  $S$  be the free shrinkage (that is,  $\epsilon_{xx} = \epsilon_{yy} = S$ , for  $0 \leq z \leq h$ ) in the plate. For the Cartesian system shown in Figure 1, the boundary conditions at the bottom face are

$$u = Sx; v = Sy; \text{ and } w = 0 \quad (1)$$

which result in

$$\epsilon_{xx} = \epsilon_{yy} = S \quad (2)$$

where

$u, v, w$  = displacements in  $x$ -,  $y$ -, and  $z$ -directions; and  
 $\epsilon_{xx}, \epsilon_{yy}$  = unit elongations in  $x$ - and  $y$ -directions.

Using Hooke's law and Eq. 2, we can express the stresses at the interface by

$$\sigma_{xx} = \sigma_{yy} = ES/(1 - \nu) \quad (3)$$

where

$E$  = modulus of elasticity of the slab material; and  
 $\nu$  = Poisson's ratio of the slab material.

Although the theoretical determination of stresses in the top of the plate is complex, Durelli (4) has solved this problem by employing photoelastic models. The stress obtained at the center of a 14-in. by 14-in. by 1-in. epoxy slab is

$$\sigma_{xx} = \sigma_{yy} \approx 2 ES \quad (4)$$

where  $\sigma_{xx}, \sigma_{yy}$  = normal components of stress parallel to  $x$ - and  $y$ -axis.

**Stress in a Free Slab**—Contrary to conditions found in a plate bonded to a rigid foundation, in an unrestrained plate the stress due to uniform shrinkage will be zero. If the shrinkage is linear but is not symmetrical with respect to the central plane, the stresses can be computed by the following expression (31):

$$\sigma_{xx} = \sigma_{yy} = -\frac{ES_z}{1 - \nu} + \frac{1}{h(1 - \nu)} \int_0^h ES_z dz + \frac{12z}{h^3(1 - \nu)} \int_0^h ES_x z dz \quad (5)$$

where  $h$  = thickness of slab.

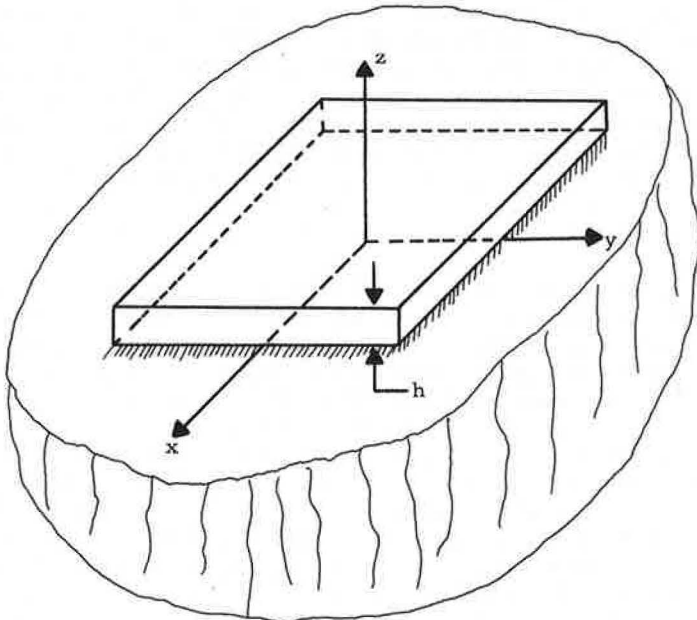


Figure 1. Slab bonded on one face and shrunk.

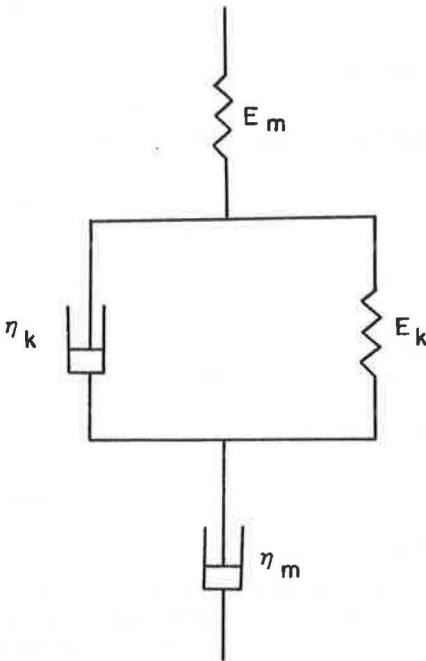


Figure 2. Rheological (Burgers) model of soil-cement for soil K03 at 6 percent cement ( $E_m = 0.89 \times 10^6$  lb/in.<sup>2</sup>;  $\eta_m = 4.50 \times 10^7$  lb-hr/in.<sup>2</sup>;  $E_k = 1.70 \times 10^6$  lb/in.<sup>2</sup>; and  $\eta_k = 1.89 \times 10^7$  lb-hr/in.<sup>2</sup>).

This discussion reveals that the stress level in a shrinking slab is primarily dependent on 2 factors: shrinkage strain distribution and subgrade restraint. The latter will be shown to depend on the former. Because both of these factors vary as the drying shrinkage progresses, a rigorous analysis of the stresses in a shrinking pavement slab can be complex. Given in the following, however, is a simplified analysis of the shrinkage stresses in a soil-cement slab permitted to dry from the top face only.

#### Theoretical Analysis of Shrinkage Stress

Before expressions for shrinkage stress can be derived, assumptions must be made in regard to laws controlling the flow of moisture in soil-cement and the relationship between shrinkage and moisture loss as well as the stress-strain-time relation. Assuming that the weight flux of water perpendicular to the direction of flow is directly proportional to the potential gradient and that the movement of water obeys the principle of conservation of matter, Gardner (6) obtained the 1-dimensional flow equation

$$\frac{\partial \theta}{\partial t} = D(\theta) \frac{\partial^2 \theta}{\partial z^2} \quad (6)$$

where

$$\begin{aligned} \theta &= \text{moisture content, percent; and} \\ D(\theta) &= \text{diffusivity, in.}^2/\text{hour.} \end{aligned}$$

The diffusivity in soil-cement, unlike that in natural soils, can be assumed to be nearly constant over a limited range of moisture change. Equation 6, with constant diffusivity, has been solved (2); a solution specifically applicable to the present problem is given by Sanan and George (27) and by Pickett (23). The shrinkage versus moisture content (weight loss) relationship has been experimentally determined (8) and found to be approximately linear except during the final stages of drying. Burgers model, as shown in Figure 2, is chosen to describe the stress-strain-time relation of soil-cement (10). These assumptions were used in computing shrinkage strain,  $S$ , in a slab drying from the top face (27), which is shown in Figure 3a. These strain distributions, at various indicated times, are exact solutions for a slab infinite in the  $x$ - $y$  plane. These curves indicate that during the early stages of drying the exposed surface is subjected to severe shrinkage strains.

The next step in the solution is to consider the base subgrade interaction problem. The theoretical model chosen for analysis employs the bending of an infinitely long slab ( $y$ -direction) of width  $B$  ( $x$ -direction) resting on homogeneous foundations whose reaction against the slab is proportional to the deflection (Winkler foundation). As a result of drying, the slab is subjected to shrinkage strain that varies nonlinearly with depth (Fig. 3a) but remains constant on any given plane parallel to the surface of the slab.

The expressions for the stresses in the  $x$ - and  $y$ -directions are given in another paper (27). Stresses on the exposed surface have been calculated by employing these equations and are plotted with time in Figure 4. The tensile shrinkage stresses attain maximum value during the early stages of drying (40 to 100 hours, depending on restraint condition) and then decrease comparatively rapidly. The maximum shrinkage stress varies from  $0.208 E_m S_\infty$  with no restraint to  $0.273 E_m S_\infty$  with complete restraint. Theoretically, regardless of the restraint condition, shrinkage stress is highly localized on the exposed surface and decreases sharply with depth (Figs. 3b and 3c). This highly localized stress can be relieved only by surface cracks or by plastic flow in the material.

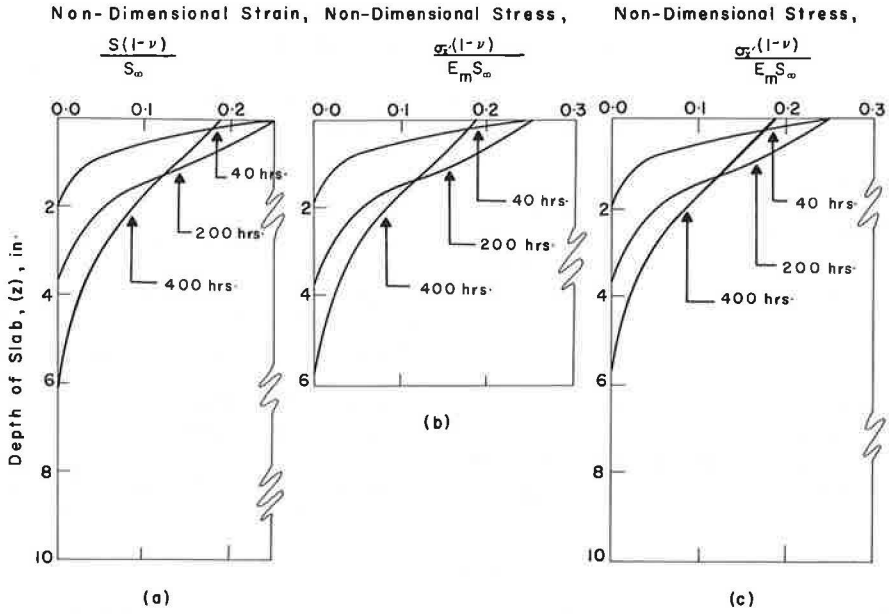


Figure 3. Shrinkage stress and strain distributions in a restrained slab at various times for soil K03-6.

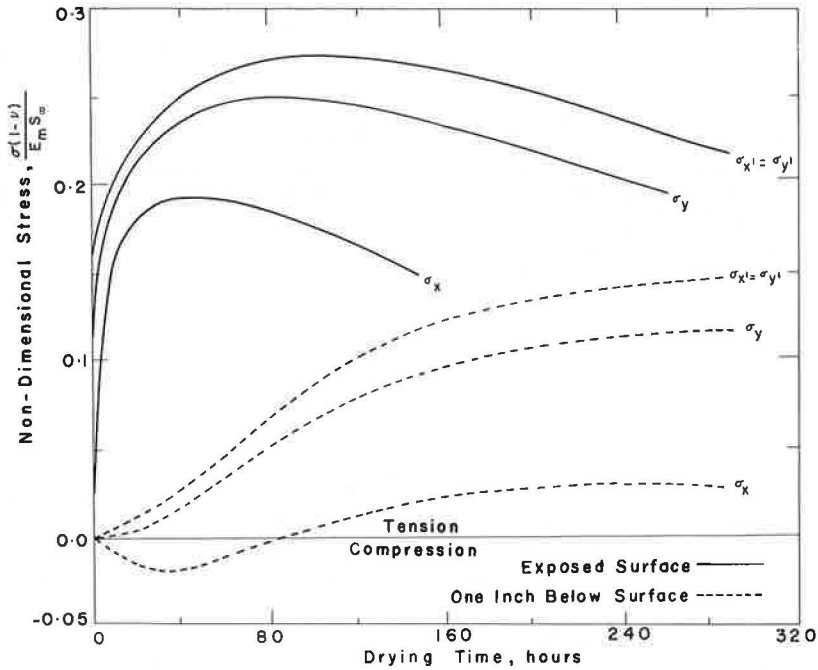


Figure 4. Variation of tensile shrinkage stress (viscoelastic) with drying time for slab 8 in. deep and for soil K03-6 ( $\sigma_{x1}, \sigma_{y1}$  = stress for complete restraint, and  $\sigma_x, \sigma_y$  = stress for no restraint).

If yielding takes place, there will be redistribution of stresses on the surface, a condition that has not been accounted for in this analysis. It may be interesting, therefore, to examine the stress variation at some interior point close to the exposed surface. The graphs shown in Figure 4 (indicated by broken lines) indicate the stress distribution at a point 1 in. beneath the exposed surface. As expected, the stress intensity decreases by 50 to 80 percent, whereas the time to attain maximum stress increases to as long as 200 to 350 hours.

In summary, the linear viscoelastic theory predicts that the shrinkage stress in a pavement slab subject to drying from one face is highly localized on the exposed surface and decreases sharply with depth. This highly localized stress can be relieved either by surface cracks or by plastic flow in the material. The limitations of the stress analysis presented should, therefore, be recognized because the 4-element model, especially at failure, does not necessarily represent the exact stress-strain-time behavior of soil cement. Furthermore, the stresses, to an important degree, are dependent on the subgrade restraint. In pavement slabs, therefore, the complex interactions among many factors involved during drying preclude a general study of the cracking until a number of gaps in the knowledge concerning these factors have been closed. For quantitative results, therefore, this investigation utilizes the techniques of dimensional analysis and scale-model experiments as described in the following section.

### SCALE-MODEL STUDIES

A model is a device that is so related to a physical system that observations on the model may be used to predict the performance of the physical system in the desired respect. Kondner (17) has previously demonstrated the effectiveness of this approach in the field of soil mechanics. Although pavement cracking is not amenable to study by a "true" model, it is highly desirable to proceed with a somewhat distorted model study.

#### Formulation of the Problem

The design of the experimental model is based on a dimensional analysis of the linear problem of shrinkage cracking. The principal advantage of dimensional analysis lies in reducing the number of variables that must be investigated and in formulating advantageous dimensionless variables.

The extent of cracking in a stabilized soil-cement base, or any pavement for that matter, can be denoted by the area of cracks,  $I$ . The important factors that affect cracking are the geometrical dimensions of the base, the stress-strain-time characteristics of the material and its tensile strength, the resistance offered by subgrade, and the rate and extent of shrinkage. The geometry of the base may be defined by its length  $L$ , breadth  $B$ , and thickness  $H$ . The base is usually cast continuously; a construction joint, however, may occur every 80 to 100 ft.

If the material can be idealized by a Maxwell fluid, the stress-strain characteristics of the base may be described by the Young's modulus  $E$  and modulus of viscosity  $\eta$ . As postulated earlier, the cracking depends on the tensile strength of the material,  $\sigma_u$ , which is assumed to remain constant throughout the test.

Subgrade interaction is a complex process. Friberg (5) has stated that, because of temperature variations or other causes, movement in the slab occurs over a certain length (called the active length) from the free end. Over a major portion of the active length the frictional resistance is constant and depends on the weight of the pavement. The resisting force in this investigation, however, is assumed to be constant over the entire length and is taken to depend on the frictional resistance per unit area per unit depth,  $F_\mu = \mu\gamma$ .

In the field, a soil-cement base is subjected to the combined effects of drying shrinkage and fluctuations of temperature. The latter, of course, influence the rate of shrinkage. In this study, however, the models are exposed to an atmosphere of constant temperature and relative humidity (RH). Even then, shrinkage strain may be a nonlinear function of time as shown in Figure 5 (10). This condition can be approximated, however, by a bilinear curve as shown in the figure. The pertinent variables, therefore,

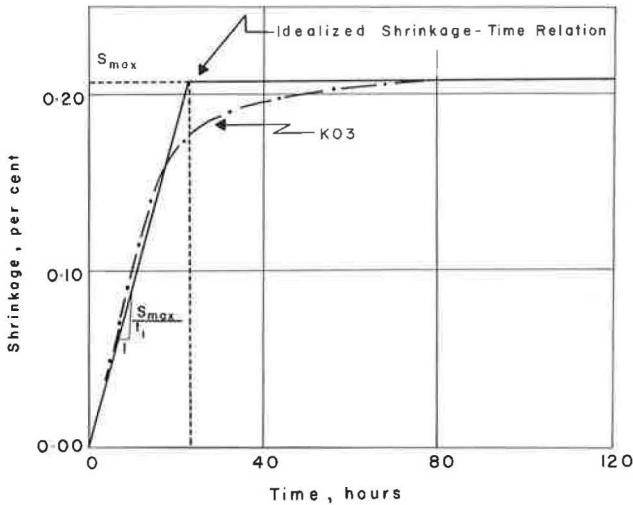


Figure 5. Typical time-rate of shrinkage of soil-cement when air-dried at 55 RH and  $72 \pm 4F$ .

may be taken as the rate of shrinkage,  $\dot{S}_{av}$ , and the time to attain maximum shrinkage,  $t_1$ . For the time being, it is assumed that the variation of shrinkage throughout the depth of the pavement does not cause any warping; what affects the phenomenon is the average shrinkage.

These considerations result in the set of physical quantities given in Table 1. There are 11 variables, and by examination it can be determined that rank of the dimensional matrix is 3. So there are 8 independent dimensionless products, which give the following functional relationship:

$$\frac{I}{LB} = f\left(\frac{B}{L}, \frac{H}{L}, \frac{E}{\sigma_u}, \frac{\eta}{HF_u t_1}, \frac{\eta}{\sigma_u t_1}, \dot{S}_{av} t_1, \frac{t}{t_1}\right) \quad (7)$$

If the material used in the model is the same as that in the prototype, by artificially treating the foundation to increase  $\mu$ , the dimensionless product  $\eta/(HF_u t_1)$  in the model may be made equal to that in the prototype. If a scale factor of  $1/10$  is chosen as the geometrical scale, the coefficient of friction should be increased 10 times.

For a particular soil,  $S_{max} (= \dot{S}_{av} t_1)$  is constant and, therefore, can be omitted from the list. Tests have to be conducted separately, however, for each type of soil. When we alter the cement content, if we assume that  $E$  is increased in proportion to  $\sigma_u$ , the factor  $E/\sigma_u$  can be taken to be constant and therefore omitted from Eq. 7.

In practice the breadth of the pavement cannot be altered to control cracking. It must be held constant. The term  $H/L$  is different from  $B/L$ , however. Changing the thickness may affect  $t_1$ ; for example,  $t_1$  increases with the thickness. Also,  $F_\mu$  may be affected by a change in thickness. Because  $H/L$  may not affect the crack intensity in a direct manner, it may be deleted from Eq. 7.

Having made the restriction that  $\sigma_\mu$  and  $\eta$  be the same in the prototype and in the model, we can satisfy the equation  $(\eta/\sigma_u t_1)_m = (\eta/\sigma_u t_1)_p$  by having  $(t_1)_m = (t_1)_p$ . This requirement was complied with by drying the experimental model in 55 percent RH. For the 3 soils tested, this requirement resulted in a drying period of approximately 15 days for the model that corresponded to the same period in the prototype. The assumption here is that under extreme field conditions the prototype pavement undergoes drying in approximately 15 days.

Using the same soil as in the prototype pavement, with the simplifications introduced and the restrictions imposed,

TABLE 1

PHYSICAL QUANTITIES CONSIDERED IN THE DIMENSIONAL ANALYSIS OF CRACKING OF SOIL BASE

Physical Quantity	Symbol	Dimension
Geometry		
Length of pavement	L	L
Breadth of pavement	B	L
Thickness of pavement	H	L
Variables controlling stress-strain-time characteristics		
Young's modulus	E	FL <sup>-2</sup>
Modulus of viscosity	$\eta$	FL <sup>-2</sup> T
Tensile strength	$\sigma_u$	FL <sup>-2</sup>
Variable affecting subgrade resistance		
Resisting force/unit area/unit depth = $\mu_v$	$F_\mu$	FL <sup>-3</sup>
Variables affecting shrinkage		
Shrinkage rate	$\dot{S}_{av}$	T <sup>-3</sup>
Time	t	T
Time to reach maximum shrinkage	$t_1$	T
Dependent variable		
Area of cracks	I	L <sup>2</sup>

we can write the functional relation for a specific soil as

$$\frac{I}{LB} = f\left(\frac{\eta}{HF_{\mu}t_1}, \frac{\eta}{\sigma_{ut_1}}, \frac{t}{t_1}\right) \quad (8)$$

### Experimental Procedure

**Materials**—Model tests were conducted in 3 soils, each at 3 to 4 different cement contents. Classification properties of these soils are given in Table 2. For convenience, each soil is identified by a 1-letter, 4-digit system; for example, K03-06 means soil with 6 percent cement whose predominant clay mineral is kaolin. Type I portland cement was used in this study.

**Model Testing**—The model of the base consists of a 4-ft by 2-ft by 1-in. thick soil-cement slab with 1 of its short edges fixed and the other 3 edges free. Simulating the subgrade underneath is an aluminum plate whose interlocking (frictional) characteristics are modified to satisfy the similitude requirements. If a geometrical scale of  $\frac{1}{10}$  is used, the model so designed simulates half of a prototype pavement slab of size 80 ft by 20 ft by 10 in. thick.

The soil-cement mixture, which has been mixed slightly above the optimum moisture, is compacted by a 45-lb roller to approximately 90 percent of the AASHO T-99 density. After casting, the slab is kept in a fog room (RH nearly 100 percent and temperature  $72 \pm 2$  F) for 7 days. After curing in the fog room, the model is dried by exposure in 55 percent RH at  $72 \pm 2$  F. The field condition is simulated by sealing all surfaces except the top face, and the slab is allowed to dry through the top face only. Cracks that appear as the slab dries eventually form a definite pattern in which orthogonal intersections predominate. The length and width of the cracks that occur as the slab dries are the important data collected from the model tests.

Rosette strain gages cemented to a corner at the free end of the model are used to measure shrinkage strain. The fact that the corner of the slab can be assumed to be stress free ensures that the creep strain and strain due to stress are both nearly zero. The shrinkage strain is thus obtained from the strain gage. (Shrinkage strain is that unit deformation due to any cause other than stress that would occur in an infinitesimal element if the element were unrestrained by neighboring elements.)

The investigation of the factors responsible for pavement cracking entails the evaluation of the crack intensity due to variation of the 3 dimensionless products on the right side of Eq. 8. Because the explicit relationship between the dependent variable and the other dimensionless products is not known, it is desirable to limit each parameter within a range consistent with the prototype pavement. The dependent parameters are varied as follows: (a)  $F_{\mu}$  by changing the frictional characteristics of the aluminum plate, (b)  $\sigma_u$  by changing the cement content in the soil, (c)  $t$  by taking measurements at various intervals, and (d)  $t_1$  by covering the surface so as to reduce the rate of drying.

When cement content of a soil is varied to change  $\sigma_u$ , both  $t_1$  and  $\eta$  change and thus affect the dimensionless factor  $\eta/(HF_{\mu}t_1)$  in Eq. 8. Experimental results, however,

TABLE 2  
SOIL CLASSIFICATION DATA

Characteristic	Sand Clay (K03)	Sand Clay (K36)	Silty Clay (M30)
Liquid limit, percent	31	22	37
Plasticity index, percent	10	1	13
-2 micron clay, percent	16	16	20
Mineral composition of -2 micron clay	Kaolinite	Kaolinite	Montmorillonite and illite
Classification			
AASHO system	A-2-4	A-2-4	A-6-9
Unified system	SM	SM	ML
Textural system	Sandy	Sandy	Silty clay



show that  $\eta/t_1$  remains nearly constant for any specific cement that ensures that Eq. 8 is the governing relation.

## RESULTS AND DISCUSSION

The experimental data from the model tests are presented here. Several tests were repeated to ensure duplicability. The crack intensity,  $i (= I/LB)$ , as defined in this report, is the unit of area of cracks per unit area of slab ( $\text{in.}^2/\text{in.}^2$ ). In reporting the crack intensity, however, weight factors such as 1, 0.8, and 0.5 are assigned respectively to initiate, lengthen, and widen a crack. These factors are semi-empirical and have been chosen so that the factor associated with each of these events is inversely proportional to the probability of its occurrence. By modifying lengthening and widening in this manner, the author hoped to obtain the crack potential of the shrinking slab. The following example illustrates how these weight factors can be used to determine a crack intensity value in a model. The increase in crack intensity,  $\Delta i$ , due to an increase in width (weight factor 0.5) from 0.02 to 0.03 in. of a 1-in. long crack (per unit area) would be  $0.005 \text{ in.}^2/\text{in.}^2$ . Adjustment of the measured crack area as indicated, however, does not change the qualitative nature of the results presented in this section.

### Graphical Representation of the Model Test Results

As indicated earlier, Eq. 8 governed the design of the model. With one exception, all of the geometric design conditions were satisfied in the model. It was not possible to reduce the size of the soil particles used in the laboratory to the same scale as the other geometrical parameters. This contradiction in geometrical similitude between the model and the prototype can be overcome by assigning an appropriate distortion factor for each soil type. Inasmuch as the principal objective of this investigation has been to delineate the factors affecting cracking, an exact numerical value for the distortion factor cannot be of great value; this discrepancy, however, precludes a direct comparison of the results of soils with different textures. The fact that a significant quantity such as  $S_{\max}$  has been deleted from the general functional relation, Eq. 8, further invalidates the scope of combining the results of fine-grained and coarse-grained

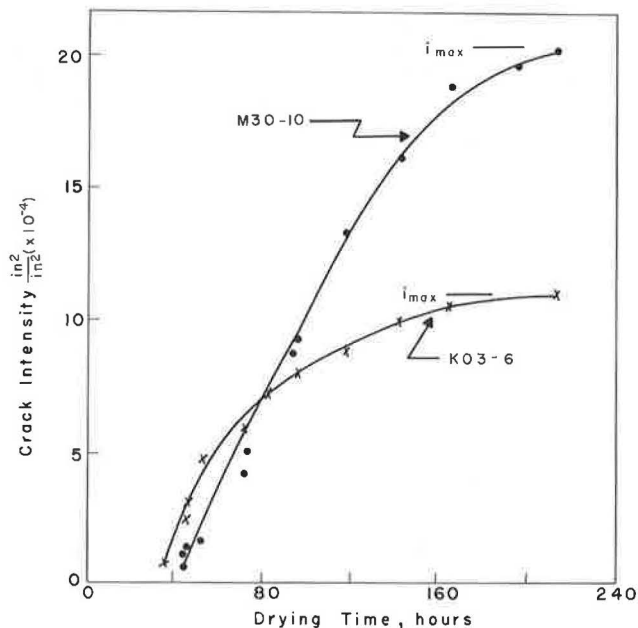


Figure 6. Typical curves of crack intensity versus drying time.

soils. Of necessity, therefore, the results of these 2 groups of soils will be analyzed separately. Because relatively more data are available for the latter group of soils, the discussion that follows will primarily concern granular soils.

Typical plots showing the increase in crack intensity with time are shown in Figure 6. The maximum crack intensity,  $i_{\max}$ , in each test has been estimated from similar plots, and its variations with the other dimensionless parameters,  $\eta/(\sigma_{II} t_1)$  and  $\eta/(HF_{II} t_1)$ , are shown in Figure 7. Because the maximum crack intensity is of interest in this study,  $t/t_1$  can be taken to be unity and, therefore, deleted from Eq. 8. The following conclusions from the plot seem warranted:

1. Crack intensity,  $i$ , increases with modulus of viscosity ( $\eta$ ), and the use of such additives as

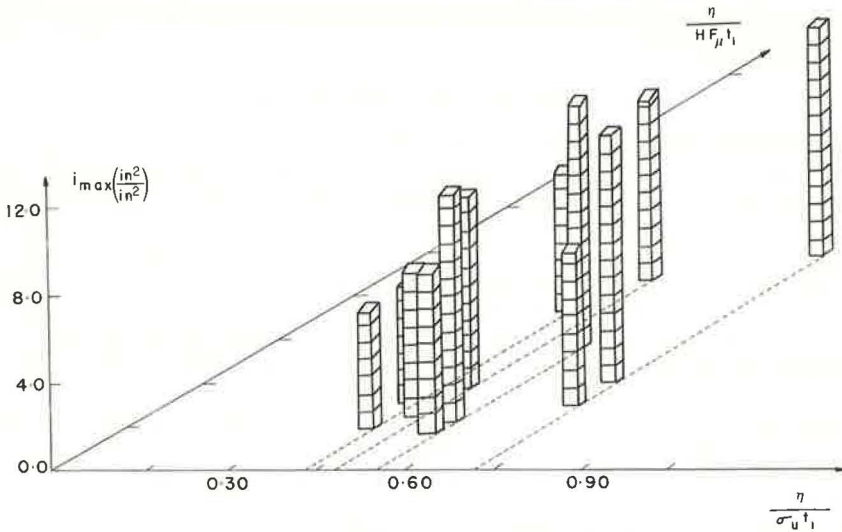


Figure 7. Crack intensity,  $i_{max}$ , related to 2 dimensionless parameters (crack intensity decreases with decrease in parameters).

emulsion or rubberized asphalt should be considered for decreasing viscosity and, therefore, minimizing cracks; and

2. Crack intensity decreases with an increase in thickness of the slab  $H$ , the time taken to attain the maximum shrinkage  $t_1$ , the tensile strength  $\sigma_u$ , and the coefficient of subgrade friction  $\mu$ .

The importance of thickness can be demonstrated by a comparison of the theoretical stress distribution in the interior of slabs 6 in. and 10 in. thick. It can be observed in Figure 3b that, when the drying time of a 6-in. slab is increased from 40 to 400 hours, the critical depth (defined as the zone in which the shrinkage stress exceeds the strength of the material) increases from 20 percent of slab depth to 60 percent. When the same time interval is observed in a 10-in. slab, however, the critical depth increases from 10 percent to only 35 percent. In other words, because tensile stress exceeds the strength, a 6-in. slab will crack more in a given time than will a 10-in. slab.

When the slab is unrestrained, however, shrinkage stress can be shown to be a function of the characteristic of the system,  $\lambda$ , where

$$\lambda = (K/4D)^{1/4} \tag{9}$$

where

$D = Eh^3/[12(1 - \nu^2)]$ ; and  
 $K = \text{modulus of the foundation.}$

It has been verified (15, 27) that warping stresses and, thereby, shrinkage stresses in an unrestrained slab decrease with an increase in the flexural rigidity,  $EI$ , or a decrease in the modulus of the foundation. In other words, tensile stresses due to warping are lowered significantly more by thick slabs on weak subgrades than by thin slabs on strong subgrades.

The significance of increasing  $t_1$ , that is, the desirability of adequate curing, is discussed elsewhere (10). The findings of that study show conclusively that cracking in cement base can be minimized by adequately extended curing. The last 2 factors, namely  $\sigma_u$  and  $F\mu$ , have been varied in the present investigation; consequently, the results and the significance of these factors on cracking are discussed in some detail.

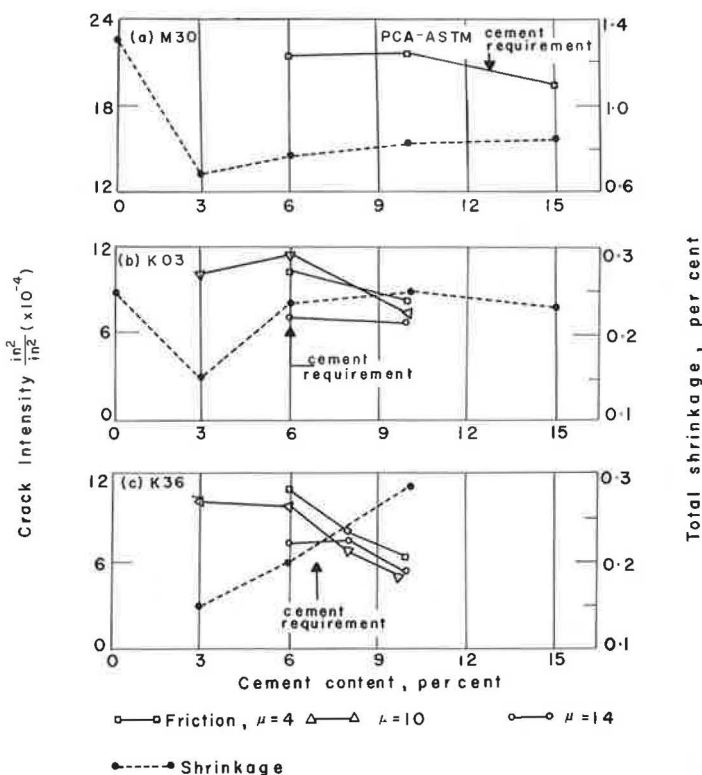


Figure 8. Variation of crack intensity with cement content in soils M30, K03, and K36 for various values of subgrade friction.

### Effect of Cement Content (Tensile Strength) on Crack Intensity

In Figure 8, the 2 curves for granular soils are shown to have certain characteristics in common. That is, for treatment levels ranging from a small percentage of cement to that specified by the Portland Cement Association (PCA) criterion (according to ASTM D 560), the crack intensity remains nearly constant. Thereafter it begins to decrease. For granular soils, therefore, it may be desirable to use slightly more cement than is required to meet the PCA-ASTM criterion.

Although cracks result primarily from shrinkage, it is paradoxical that the crack intensity results do not agree with the shrinkage results reported in a previous study (9). Typically, as shown by broken lines in Figures 8b and 8c, the minimum shrinkage occurred in cement proportions somewhat below the PCA requirement; thereafter shrinkage increased as cement content was increased. At low cement contents, although shrinkage is at a minimum, the base, on account of its low tensile strength, tends to exhibit closely spaced cracks. Conversely, when cement content is increased, tensile strength is also increased and cracks occur at wider spacings. The increased crack spacing can be shown to have a twofold effect on crack width and, therefore, on crack intensity. First, as evidenced by the equation (7)

$$\delta_Y = S_{\infty}L - \frac{\mu\gamma L^2}{4E_t}$$

where

$\delta_Y$  = crack width,

- $S_{\infty}$  = maximum (final) shrinkage,  
 $L$  = crack spacing,  
 $\mu$  = coefficient of subgrade friction,  
 $\gamma$  = unit weight of base, and  
 $E_t$  = Young's modulus in tension,

crack width decreases with  $L^2$ . Second, as shown by Pickett (22), the creep strain, which arises from the restraint in the slab, increases with slab size and partly compensates for the shrinkage, thereby reducing the crack width. In summary, the higher tensile strength overcomes the adverse effect of increased shrinkage.

The crack intensity in the fine-grained soil, M30, is nearly constant with the increase in cement content, a fact in satisfactory agreement with the shrinkage results (Fig. 8a). In fine-grained soils, a cement content that meets the PCA-ASTM criterion should give a satisfactory mix for design purposes.

### Effect of Subgrade Friction on Crack Intensity

In the fine-grained soil, the crack intensity remains unchanged, whereas in the 2 coarse-grained soils, as shown in Figure 7, the crack intensity tends to decrease with  $\mu$ . In explaining these results, it may be noted that crack intensity is influenced by 2 opposing factors. As  $\mu$  increases, frictional resistance increases (7, Eq. 1a) creating frequent cracks. The data given in Table 3, which show that the crack length increases with increase in  $\mu$ , support this hypothesis and perhaps suggest an increase in crack intensity as well. The increased restraint, however, opposes this tendency, as it enhances the creep in the shrinking matrix and partly compensates for the shrinkage to reduce the crack width and, thereby, crack intensity. The effect of subgrade will be even more significant in the field. That is, the high frictional resistance may serve to redistribute more evenly the stresses caused by localized shrinkage and, thereby, reduce the incidence of cracking. The theoretical studies of Pickett (22) as well as the experimental results obtained by Nagataki (20) show that as restraint increases the resultant strain assumes nearly uniform distribution.

The fact that crack intensity in the fine-grained soil model is not significantly influenced by the subgrade resistance can be the result of warping in cracked panels. As drying of the model slab continued, cracks appeared. After further drying at constant temperature, these cracked panels separated out of the base and exhibited large convexity at the top face (11). It was concluded, therefore, that crack intensity during the later stage of drying cannot be a function of the subgrade resistance.

Test results indicate that increasing the subgrade friction tends to reduce crack intensity. The observation that mixed in-place jobs exhibit less cracking than do central plant jobs validates this finding.

### Cracking Influenced by Texture of Soil

By necessity, the gradation or texture of soil is not taken into consideration in designing the model. It does not seem feasible, therefore, to relate crack intensity to textural characteristics such as clay content. Indirectly, however, a relation can be demonstrated here. The effect of clay content on shrinkage has been reported (9), and the results show that the shrinkage increases somewhat exponentially with -2 micron clay content.

From the results of the present investigation, it can be shown that crack intensity is influenced by shrinkage. As given in Table 4, for example, the crack intensity increases somewhat proportionally with the drying shrinkage. It must be emphasized that, of all factors pertaining to soil, the clay exerts the most influence in cracking of soil-cement base.

TABLE 3  
ULTIMATE CRACK LENGTH OBSERVED IN MODEL

Soil	Cement (percent)	Length of Cracks <sup>a</sup> (in.)		
		$\mu = 4$	$\mu = 10$	$\mu = 14$
K03	3	79.5 (30.5)	91.0 (29.5)	
	6	63.0 (35.0)	84.0	
	10	25.0 (21.5)	35.0 (28.0)	34.5 (26.5)
K36	6	66.0	54.0	
	8	43.0	35.0	
	10	44.0	41.5	70.0
M30	6	103.5		113.0
	10			
	15	64.0		103.0

<sup>a</sup>Maximum shrinkage strain,  $S_{\infty} \times 10^{-4}$ , is in parentheses.

The effect of coarse aggregates in cracking is somewhat understood. By acting as rigid inclusions in the shrinking matrix, they reduce shrinkage (9, 24). The part played by the gravel, approximately  $\frac{1}{2}$  to  $1\frac{1}{4}$  in. nominal size, often found in cement-treated clay-gravel mixtures, is discussed in the following.

A recent study (29) on the shrinkage microcracking in concrete reveals that tensile stresses, developing at the aggregate-cement paste interface, cause microcracks at the interface during the curing period of concrete.

Several studies concerning the disturbing effect of small spherical and cylindrical inclusions on an otherwise uniform stress distribution are reported in the literature (3, 13, 28). In simple tension, for example, a perfectly rigid spherical inclusion intensifies the tension at the "poles," in the same direction as the applied tension  $T$ , to about  $2T$  (13).

Aggregates, therefore, assume a dual role in the shrinkage cracking of soil-cement: First, by acting as rigid inclusions in the shrinking matrix, they inhibit shrinkage; and, second, by virtue of the stress concentration at the interface, they tend to enhance cracking. This problem has been investigated by model testing.

Inasmuch as the model design followed the principles of dimensional analysis, it was desirable to proportion the aggregate size accordingly. It is shown elsewhere (13) that stresses in 2 systems (model and prototype), with inclusions of the same form but different sizes, are the same at similarly situated points. A requirement in the model design that the shrinkage stresses in the model and in the prototype be the same at homologous points makes it imperative that gravel of the same size be used in the 2 systems.

Because of practical considerations, however, natural gravel of nominal size— $\frac{1}{2}$  to  $\frac{3}{4}$  in.—is used in this investigation. The gravel was randomly embedded in the M30-10 matrix at distances of approximately 10 in.

In accordance with the theory, cracks began to appear radially from the gravel inclusion. After further shrinkage, however, cracks radiating from adjacent inclusions became interconnected, resulting in the crack pattern shown in Figure 9. The presence of gravel substantially increased the cracking. For example, as given in Table 5, the crack intensity in a model with 15 pieces of gravel is 50 percent more than that in a control model containing no gravel.

A few qualitative conclusions pertaining to the effect of gravel can be drawn from the studies of Daniel and Durelli (3) and Shelly and Yuan (28). For instance, the higher the drying shrinkage is, the higher will be the stress concentration with gravel inclusions. Although the stress distribution around a single inclusion is independent of size, it can become significant when a group of inclusions is considered. The stress level is also modified by the spacing of inclusions; the smaller the spacing is, the larger will be the hoop stress evaluated at some point between the inclusions.

TABLE 4

CRACK INTENSITY COMPARED WITH MAXIMUM SHRINKAGE

Soil	Cement (percent)	Maximum Unit Shrinkage (percent)	Crack Intensity (in. <sup>2</sup> /in. <sup>2</sup> × 10 <sup>-3</sup> )
K03	6 <sup>a</sup>	0.2407	11.38
K36	6	0.2071	9.86
M30	10	0.7506	21.52

<sup>a</sup>Cement based on dry weight of soil, as a percentage.



Figure 9. Crack pattern in gravel-embedded model for soil M30-10 (location of gravel shown by circles).

## INFLUENCE OF ADDITIVES ON CRACKING

In the preceding part of this report, a number of factors regulating shrinkage cracking of stabilized pavement systems have been evaluated. Cracking can best be controlled, however, by minimizing shrinkage of the treated soil. The effectiveness of additives and treatments in reducing cracking is brought into focus in the following discussion.

### Effect of Lime

In soil-cement blends, lime replaced an equal amount of cement. As given in Table 5, 3 percent lime in K03-6 and K36-6 and 4 percent lime in M30-10 reduced the crack intensity by 60, 65, and 25 percent respectively. This reduction is in excellent agreement with the shrinkage results reported by George (7). The addition of a small proportion of lime reduced the shrinkage in several soils by 30 to 40 percent. The fact that lime flocculates clay more effectively than cement and facilitates better compaction is another point in favor of recommending lime in cement-treated soils, especially in fine-grained soils. In proportioning the lime, it should be kept in mind that the compressive strength of a lime-soil-cement mixture is slightly less than that of a soil-cement mixture of equivalent cement content.

### Effect of Lime and Sugar

It is generally agreed that early setting of cement is detrimental (9); therefore, it may be desirable to use slow-set cement in soil-cement work. Zube et al. (33) have reported that Type II cement, because of its slow set rate, is better than Type I cement in preventing block cracking. Orchard (21) and Arman (1) advocate the use of retarding admixtures in soil-cement.

The author of this study experimented with a trace amount of sugar in soil-cement-lime mixtures, and the crack intensity result is given in Table 5. The response of the 2 granular soils tested is remarkable. Even with 2 percent lime and  $\frac{3}{8}$  percent sugar, crack intensities in K03-6 and K36-6 were reduced by 67 and 65 percent respectively. As little sugar as  $\frac{3}{16}$  percent has been found to be effective in K03.

The reduction of cracks in sugar-treated models can be attributed to the reduced shrinkage rate of the material. As recorded by the strain gages, the shrinkage rate in

TABLE 5  
EFFECT OF ADDITIVES ON CRACK INTENSITY

Additive	Additive Concentration (percent)	Crack Intensity (in. <sup>2</sup> /in. <sup>2</sup> × 10 <sup>-4</sup> )		
		Soil K03	Soil K36	Soil M30
Gravel	Cement 10; $\frac{1}{2}$ to $\frac{3}{4}$ in. nominal size gravel			33.50
	Cement, 10 (control)			21.52
Lime	Cement, 6; lime, 3	3.33	2.29	
	Cement, 10 (control)	8.33	6.66	
Lime	Cement, 10; lime, 4			14.43
	Cement, 15 (control)			19.26
Lime and sugar	Cement, 6; lime, 2; sugar, $\frac{3}{8}$	2.74	3.44	
	Cement, 10 (control)	8.33	6.66	
Expansive cement	Cement, 0; expansive cement, 10	0.38		22.36
	Cement, 5; expansive cement, 5	0.52		22.85
	Cement, 10 (control)	8.33		21.52
Sodium metasilicate	Cement, 6; 5 percent sodium metasilicate solution applied $\frac{7}{10}$ gal/sq yd	2.50		
	Cement, 6 (control)	10.34		

sugar-treated models was reduced on the order of 40 percent from that in the untreated models. Previous studies (10, 27) have shown conclusively that shrinkage stresses and, thereby, cracks can be reduced by decreasing shrinkage rate.

When the compressive strengths were compared, it was found that, if  $\frac{3}{8}$  percent sugar is added, the 7-day compressive strengths in K03-6 and K36-6 were reduced by 80 and 77 percent respectively. It is significant, however, that sugar-treated mixtures, if adequately cured, will develop strengths nearly equal to their untreated counterparts.

### Effect of Expansive Cement

The primary use of expansive cement in concrete or soil-cement is to expand and compensate for the shrinkage that occurs during drying. Besides compensating for shrinkage, the mechanical behavior of a pavement base, which normally is continuous or restrained at the bottom or both, can be significantly modified by the expansion. If the cement base is restrained while the expansive soil-cement is curing and tending to expand, a compressive stress can be built up within the soil-cement. The experimental finding of Nagataki (20) supports this hypothesis. Upon drying, the soil-cement, which would shrink without the prior restraint, would be relieved of the compressive stress developed during the curing period. In other words, if the base material is prestressed, ultimate tensile capacity is increased by the same order of magnitude, thereby eliminating most of the shrinkage cracks.

The crack intensity in the 2 soils with varying amounts of expansive cement (expansive cement replaced an equal amount of portland cement) is given in Table 5. The results indicate that with 10 percent expansive cement in K03 (typical of a coarse-grained soil) the crack intensity is reduced by 90 percent. In fine-grained montmorillonite soil, M30, however, the expansive cement is not effective. This finding agrees with the reported results (7) in that, by replacing 50 percent of the portland cement with an equal amount of expansive cement, the shrinkage was reduced in 5 out of 7 soils tested; all 5 soils were coarse-grained soils. The test results, although limited, indicate that shrinkage can be substantially reduced by replacing approximately 50 percent of the portland cement by expansive cement. Fine-grained soils are not generally responsive to expansive cement.

### Surface Hardening of Soil-Cement

As shown in Figure 3b, the shrinkage stress is highly localized; as a result, cracks originate on the exposed surface. A simple expedient to control surface cracking, therefore, would be to increase the hardness of the upper crust. Some early work on surface hardening of stabilized soil has been reported by Handy et al. (14). They showed that only a 5 percent solution of sodium metasilicate applied in the amount of  $\frac{1}{2}$  gal/sq yd approximately doubled the bearing strength. In this investigation 5 percent sodium metasilicate solution was sprayed in 2 equal installments at the rate of 0.3 gal/sq yd. The result was striking in that the crack intensity in K03-6 was reduced by 66 percent.

The reduction in crack intensity can be attributed primarily to 2 factors. First, because the silicate treatment boosts the surface hardness, as critical stresses occur at the exposed surface, the top-reinforced base is especially resistant to surface cracking. Second, by virtue of its ability to diffuse uniformly through the pore fluid (18), sodium metasilicate lowers the diffusivity coefficient,  $k$ , and thereby the evaporation rate. ( $k$  is a measure of the amount of moisture moving through a unit volume of the material in unit time.) The results of this study as well as those of a previous study (10) showed that by lowering the evaporation rate the incidence of cracking can be minimized.

### Effect of Moisture and Density

Results concerning the effect of moisture and density on shrinkage have been reported by the author (9). They are as follows:

1. Compaction at wet or optimum moisture content results in appreciably higher total shrinkage, and molding moisture appears to have the most influence on shrinkage; and

## 2. Shrinkage can be reduced by improving compaction.

Because the model design was based on a dimensional analysis of the linear problem, the effect of moisture content on crack intensity in the prototype pavement cannot be predicted from model studies. Some approximate calculations, however, show that a 1 percent increase in moisture content in the field may result in as much as a 15 to 25 percent increase in the crack intensity. The writer emphasizes, therefore, that of all the factors molding moisture has the greatest influence on crack intensity. In the interest of brevity, detailed results of this study are not reported here. It has been demonstrated, however, that the maximum density attainable should be specified in the field in an effort to substantially reduce the crack intensity.

## SUMMARY AND CONCLUSIONS

Employing linear viscoelastic theory, the author has presented expressions whereby stresses in base slabs subject to ambient moisture gradient can be computed. As a result of this analysis, the following results seem warranted:

1. Theoretically, shrinkage stress is highly localized on the exposed surface and decreases sharply with depth;
2. The tensile shrinkage stress on the exposed surface of a soil-cement slab attains maximum value during the early stages of drying (40 to 100 hours depending on the restraint condition) and then decreases rapidly; and
3. The maximum shrinkage stress, which typically varies from 0.2 to 0.3  $E_m S_{\infty}$ , is much greater than the tensile strength of soil-cement in normal use; consequently, the surface of the slab will crack or flow under stress.

Application of these results would suggest that, if cracking is minimized, a soil-cement base warrants special attention and curing during the first critical 2 to 4 days.

The shrinkage cracking of soil-cement base was investigated by using a model whose design was based on a dimensional analysis of the linear problem of shrinkage cracking. The results are as follows:

1. The crack intensity,  $i$  (defined as area of cracks per unit area), decreases with an increase in the thickness of the slab, cement content, and the coefficient of subgrade friction;
2. The crack intensity decreases with a decrease in the modulus of viscosity of the soil and the shrinkage rate;
3. The crack intensity increases with the type and amount of clay-sized particles in the soil (clay content exerts more influence on cracking than does any other factor); and
4. Large aggregates (nominal size  $\frac{1}{2}$  in. and larger), by virtue of their ability to intensify the stress in the shrinking matrix, enhance crack intensity.

As a result of this study, it is recommended that cement equal to or slightly in excess of that required to meet the PCA-ASTM criterion be used.

The search for treatments to reduce cracking led to several promising additives. Lime and lime with a trace amount of sugar proved to be the best in a variety of soils. Expansive cement admixture and sodium silicate surface treatment are effective in well-graded, coarse-grained soils. The effect of moisture content on shrinkage cracking is sufficient to warrant a special effort to compact the soil-cement at or below, but never above, the optimum moisture. The model studies confirm that shrinkage cracking can be reduced by improving compaction.

## NOTATION

The following notations were used in this paper.

- D = flexural rigidity;
- E = Young's modulus;
- $E_K$  = Young's modulus in Kelvin model;
- $E_m$  = Young's modulus in Maxwell model;
- f = surface factor;



- $G_K$  = shear modulus in Kelvin model;  
 $G_m$  = shear modulus in Maxwell model;  
 $h$  = thickness of the slab;  
 $k$  = diffusivity coefficient of shrinkage;  
 $K$  = bulk modulus;  
 $B$  = width of slab in x-direction;  
 $S$  = free, unrestrained linear shrinkage;  
 $S_{av}$  = average shortening per unit length;  
 $S_\infty$  = final shrinkage, value of  $S$  when  $t = \alpha$ ;  
 $t$  = time;  
 $u, v, w$  = displacements in x-, y-, z-directions;  
 $\eta_K$  = modulus of viscosity in Kelvin model;  
 $\eta_m$  = modulus of viscosity in Maxwell model;  
 $\nu$  = Poisson's ratio;  
 $\theta$  = moisture content by weight;  
 $\sigma_{xx}, \sigma_{yy}$  = normal components of stress parallel to x- and y-axes;  
 $\epsilon_{xx}, \epsilon_{yy}$  = stress-induced unit elongations in x- and y-directions;  
 K03-06 = soil 3 with 6 percent cement, predominant clay mineral kaolin;  
 K36-06 = soil 36 with 6 percent cement, predominant clay mineral kaolin; and  
 M30-10 = soil 30 with 10 percent cement, predominant clay mineral montmorillonite.

#### ACKNOWLEDGMENTS

This report is part of the research conducted in connection with Project 5666 of the Engineering Experiment Station, University of Mississippi, under the sponsorship of the Mississippi State Highway Department and the U. S. Department of Transportation, Federal Highway Administration. This support is gratefully acknowledged. The opinions, findings, and conclusions expressed in this publication are those of the author and not necessarily those of the state highway department or the Federal Highway Administration.

#### REFERENCES

1. Arman, A., and Dantin, T. J. The Effect of Admixtures on Layered Systems Constructed With Soil-Cement. Highway Research Record 263, 1969, pp. 69-80.
2. Carslaw, H. S., and Jaeger, J. C. Conduction of Heat in Solids. Oxford Univ. Press, New York, 1959.
3. Daniel, I. M., and Durelli, A. J. Shrinkage Stresses Around Rigid Inclusions. Experimental Mechanics, Vol. 2, 1962, pp. 240-244.
4. Durelli, A. J., and Parks, C. J. R. Stresses in Square Slabs, With Different Edge Geometries, When Bonded on One Face to a Rigid Plate and Shrunk. Experimental Mechanics, Vol. 7, 1967, pp. 481-484.
5. Friberg, B. F. Frictional Resistance Under Concrete Pavements and Restraint Stresses in Long Reinforced Slabs. HRB Proc., Vol. 33, 1954, pp. 167-184.
6. Gardner, W. R. Mathematics of Isothermal Water Conduction in Unsaturated Soil. HRB Spec. Rept. 40, 1958, pp. 78-87.
7. George, K. P. Cracking in Cement-Treated Bases and Means for Minimizing It. Highway Research Record 255, 1968, pp. 59-71.
8. George, K. P. Criteria for Strength and Shrinkage Control of Cement-Treated Bases. Engr. Exp. Station, Univ. of Mississippi, Oxford, Research Rept., 1968.
9. George, K. P. Shrinkage Characteristics of Soil-Cement Mixtures. Highway Research Record 255, 1968, pp. 42-58.
10. George, K. P. Cracking in Pavements Influenced by Viscoelastic Properties of Soil-Cement. Highway Research Record 263, 1969, pp. 47-59.
11. George, K. P., and Prasad, S. N. Shrinkage Deformation in Panels of Cracked Pavements—A Paradox. Engr. Exp. Station, Univ. of Mississippi, Oxford, 1970.
12. George, K. P. Theory of Brittle Fracture Applied to Soil-Cement. Jour. Soil Mech. and Found. Div., Proc. ASCE, Vol. 96, May 1970, pp. 991-1010.
13. Goodier, J. N. Concentration of Stress Around Spherical and Cylindrical Inclusions and Flaws. Trans. ASME, Vol. 55, 1933, pp. 39-44.

14. Handy, R. L., Jordan, J. L., Manfre, L. E., and Davidson, D. T. Chemical Treatments for Surface Hardening of Soil-Cement and Soil-Lime-Fly Ash. *HRB Bull.* 241, 1960, pp. 49-66.
15. Harr, M. E., and Leonards, G. A. Warping Stresses and Deflections in Concrete Pavements. *HRB Proc.*, Vol. 38, 1959, pp. 286-321.
16. Kennedy, T. W., and Hudson, W. R. Application of the Indirect Tensile Test to Stabilized Materials. *Highway Research Record* 235, 1968, pp. 36-48.
17. Kondner, R. L., and Edwards, R. J. The Static and Vibratory Cutting and Penetration of Soils. *HRB Proc.*, Vol. 39, 1960, pp. 583-604.
18. Lambe, T. W., Michaels, A. S., and Moh, Z. C. Improvement of Soil-Cement With Alakli Metal Compounds. *HRB Bull.* 241, 1960, pp. 67-108.
19. Marshall, T. J. Some Properties of Soil Treated With Portland Cement. Council of Scientific and Industrial Research Organization, Australia, 1954.
20. Nagataki, S. Shrinkage and Shrinkage Restraints in Concrete Pavements. *Jour. Struct. Div., Proc. ASCE*, Vol. 96, No. ST7, July 1970, pp. 1333-1358.
21. Orchard, O. F., O'Brien, T. I., and Erwin, R. F. The Effect of Retarders on Soil-Cement Mixtures. *Proc. Permanent Internat. Assn. of Road Congresses*, Tokyo, Nov. 1967.
22. Pickett, G. The Effect of Change in Moisture-Content on the Creep of Concrete Under a Sustained Load. *ACI Jour., Proc.* Vol. 38, 1941.
23. Pickett, G. Shrinkage Stresses in Concrete. *ACI Jour., Proc.* Vol. 42, 1946, pp. 165-204.
24. Pickett, G. Effect of Aggregate on Shrinkage of Concrete and a Hypothesis Concerning Shrinkage. *ACI Jour., Proc.* Vol. 27, 1956, pp. 581-590.
25. Prandi, E. Investigation of Cracking of Gravel-Sand Mixtures Treated With Granulated Clay. *Bull. de Liaison Des Laboratoires Routieres Ponts et Chaussées.*
26. Reddy, A. S., Leonards, G. A., and Harr, M. E. Warping Stresses and Deflections in Concrete Pavements: Part III. *Highway Research Record* 44, 1963, pp. 1-24.
27. Sanan, B. K., and George, K. P. Viscoelastic Shrinkage Stress in Soil-Cement Base. Paper submitted to ASCE for publication, 1970.
28. Shelley, J. F., and Yu, Yi-Yuan. The Effect of Two Rigid Spherical Inclusions on the Stresses in an Infinite Elastic Solid. *Trans. ASME*, Vol. 88, 1966, pp. 68-74.
29. Theocaris, P. S., and Konfopoulos, T. Photoelastic Analysis of Shrinkage Microcracking in Concrete. *Magazine of Concrete Research*, Vol. 21, No. 66, 1969, pp. 15-22.
30. Thomlinson, J. Temperature Variations and Consequent Stresses Produced by Daily and Seasonal Temperature Cycles in Concrete Slabs. *Conc. and Construct. Eng.*, 1940.
31. Timoshenko, S., and Goodier, J. N. *Theory of Elasticity.* McGraw-Hill, New York, 1951, p. 401.
32. Westergaard, H. M. Analysis of Stresses in Concrete Pavements Due to Variations of Temperature. *HRB Proc.*, Vol. 6, 1926, pp. 201-207.
33. Zube, E., Gates, C. G., Shirley, E. C., and Munday, H. A. Service Performance of Cement-Treated Bases as Used in Composite Pavements. *Highway Research Record* 291, 1969, pp. 57-69.

## Discussion

J. B. METCALF, Australian Road Research Board, Victoria—The author has produced a most interesting analysis of cracking in soil cement slabs. However, I do not believe the problem he has tackled to be the central problem in stabilization. In taking the problem of cracking density, he produces arguments that show reduced cracking density with higher cement contents, i.e., with higher strengths. Yet, this is the condition that leads to the worst form of cracking, and I submit that the form of cracking is more important than its intensity as suggested here. The most common cause of failure due to cracking is the appearance of widely spaced, wide cracks in cement stabilized pavements. For this condition, the cracking density may be quite low and the strength quite high, and this is to be avoided. The first question for George is, Can

he reorient his approach to produce estimates of crack width and crack spacing rather than cracking intensity and point the direction in which cement content and so on should be moved to minimize this. I would expect to find the reverse of his present conclusions. The second question is of a rather more detailed nature: Can he provide information on the proportion of cracking due to cement hydration, rather than to drying out, because good construction practice would lead to a minimum of drying out?

K. P. GEORGE, Closure—The writer appreciates the interesting comments presented by Metcalf. Despite the apparent disagreements, the writer finds that the comments are essentially the same as those presented in the paper.

The answer to Metcalf's first question may be seen in the paper in the section entitled "Effect of Cement Content (Tensile Strength) on Crack Intensity." Should the shrinkage data, similar to those shown in Figure 8 of the paper, be the criterion, the writer tends to agree with Metcalf's hypothetical conclusions. Nevertheless, the model study shows that, for treatment levels at or slightly above the PCA-ASTM criterion, the crack spacing is increased and the crack width is decreased (in Metcalf's terminology, widely spaced, narrow cracks). The writer, therefore, would like to reaffirm his conclusion that for granular soils it may be desirable to use slightly more cement than is required to meet the PCA-ASTM criterion.

For an answer to the second question raised by the reviewer, it would be pertinent to refer to the results given in another report (9). In that report, the writer showed that the cement in soil-cement takes up moisture to result in self-desiccation and shrinkage of the order of 17 percent of the maximum shrinkage. A conclusion, based on this result, would be that perhaps 15 to 20 percent of the cracking results because of cement hydration.